International Journal of Scientific Engineering and Technology (ISSN : 2277-1581)
Volume No.2, Issue No.7, pp : 656-664 1 July 2013

Wavelet Enveloped Power Spectrum and Optimal Filtering For Fault Diagnosis in Gear

M. Lokesha[1]*, Manik Chandra Majumder[2], K. P. Ramachandran[3], Khalid Fathi Abdul Raheem[4]
[1, 3] Department of Mechanical Engineering, Caledonian College of Engineering, OMAN,
[2] Department of Mechanical Engineering, National Institute of Technology, Durgapur, INDIA,
[4]Department of Mechanical Engineering, Sohar University, OMAN
Corresponding author email: lokjay251@yahoo.com

***Abstract** -The methodology of vibration based condition monitoring technology has been developing at a rapid stage in the recent years suiting to the maintenance of sophisticated and complicated machines. The ability of wavelet analysis to efficiently detect non-stationary, non-periodic, transient features of the vibration signal makes it a demanding tool for condition monitoring. In this paper, the vibration condition monitoring based on Laplace and Morlet wavelet enveloped power spectrum analysis to detect the faults in gears is presented. The experimental studies were conducted on the gear testing apparatus to obtain the vibration signal from a healthy gear and a faulty gear. The vibration signals obtained were filtered to enhance the signal components before the application of wavelet analysis. A study detailing features of fault characterization is also given in order to understand the effectiveness of signal processing methods.*

Keywords-Continuous wavelet transform, Envelope power spectrum, Wavelet, Filtering.

I. Introduction:

With the continuous development, global competition has forced modern industries to improve production efficiency and product quality, as a result machineries are more complicated. The need for effective maintenance of these machines is of great importance in order to ensure failure free operation.

Industrial machines consist of gear box for transmission of power and variation of speed. The condition monitoring of the machine with a reliable system can identify the fault at an early stage in order to avoid any failure in the machines[1].The normal gear defects include the presence of crack in one or more of the gear tooth, chipping of teeth, geometrical imperfection etc. Vibration based condition monitoring techniques is commonly used for the fault detection and diagnosis in mechanical components like gears, bearings etc. [2,3].Machine parts develop a specific vibration signature and even a slight change in their condition will reflect the corresponding change in their vibration signature. The changes in the vibration signature can be used to identify the source of the defect using vibration analysis [4].To analyze vibration signals different techniques such as time domain, frequency domain and time–frequency domain techniques are commonly used [5-7]. The impacts produced by the faulty gear may result in non-stationary signal due to transient modification of the vibration signals and these non-stationary components contain abundant information about machine faults; therefore, it is important to analyze the non-stationary signals [8-9]. The non-stationary nature of the signal suggests the use of time-frequency techniques, which make it possible to look at the time evolution of the signal's frequency content [8,9]. FFT based condition monitoring techniques are not suitable for non-stationary signal [10].

The wavelet transform (WT) provides powerful multi-resolution analysis in both time and frequency domains and hence becomes a favoured tool to extract the transient features of non-stationary vibrations signals produced by the faults. Wavelet analysis provides better results compared to Fast Fourier Transform (FFT) spectrum[11-13].Wavelet coefficients, which are obtained by the wavelet analysis indicate the correlation of the signal with the particular wavelet. In order to extract the fault features of the signal more effective appropriate wavelet base function should be selected [14,15].The gear and rolling bearing elements faults features are extracted using Morlet and Impulse wavelet analysis. Based on maximum kurtosis concept, the wavelet features are optimized to enhance the fault detection process [16-18]. Laplace wavelet is a complex, single sided damped exponential formulated as an impulse response of a single mode system to be similar to data features commonly encountered in health monitoring tasks. It has been applied to the vibration analysis of an aircraft for aerodynamic and structural testing [20] and to diagnose the wear of the intake valve of an internal combustion engine [19].

The performance of the fault diagnosis methods are affected by the corrupting noise. The success of gear fault detection depends on signal to noise ratio. Signal processing is a method to enhance the signal by removing the noise buried in signal, thus increasing the signal to noise ratio. To perform this, an effective de-noising method would be necessary to remove such corrupting noise. Wavelet threshold-based [21,22] and wavelet filter-based [23-26] are the two techniques used to purify the vibration signals measured from faulty gears or bearings. The thresholding techniques applies the concept of thresholding rule to shrink the wavelet coefficients used in the reconstruction process [27, 28] and the wavelet filter technique applies the filtering characteristic of the wavelet transform at a fixed scale [29,30].The wavelet parameters are important for the application of de-noising techniques [32]. Adaptive noise canceller and adaptive line enhancement technique using Least mean square (LMS) and Recursive least square (RLS) algorithms are used for the effective diagnosis of rolling element bearing faults. Both LMS and RLS are effective for de-noising. However, the convergence of RLS is faster than LMS algorithm for fault features pattern identification for the bearing vibration signals [33].The Wiener filter based on the spectral kurtosis is used for the optimal filtering of gear signals. Spectral kurtosis (SK) *residual* define the local power as the smoothed squared envelope, which reflects both the energy and the degree of non-stationary of the fault-induced transients. The adjustment of the resolution for the SK estimation appears to be optimal when the length of the analysis window is approximately matched with the mesh period of the gear. [34]

In this paper, Wiener filter is used to enhance the signal components in the vibration signal and wavelet envelope power spectra is used to detect localized gear tooth defects. Also the wavelet parameters are optimized so as to maximize the kurtosis of the wavelet coefficients in order to render the wavelet coefficients sensitive to the generated fault signals. Experimental data setups which are representatives of localized gear tooth defect are used to develop the wavelet envelope power spectrum computed using Morlet and Laplace wavelet functions.

This paper is organized as follows: section 2 covers theory on the wiener filter and wavelet transform, section 3 explains the experimental setups and procedure, section 4 discusses the implementation of the enveloped wavelet power spectrum for gear fault detection and the conclusions are presented in section5.

II. Filter and Enveloped wavelet power spectrum:

2.1 Optimal signal processing: wiener filters

The Wiener filter theory works on the concept of minimizing the difference between the filtered output and desired output and it uses least mean square approach to minimize, which adjusts the filter coefficients to reduce the square of the difference between the desired and actual waveform after filtering.

The Wiener filter approach is outlined in Figure 1.

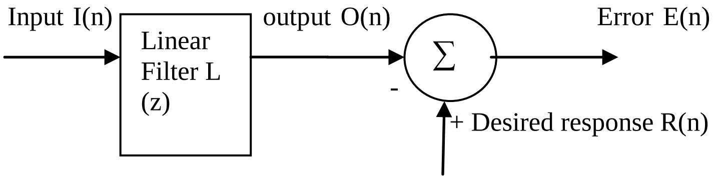

Figure 1: Wiener filter

The linear process L(z) operates the input waveform I(n) containing both signal and noise using finite impulse response (FIR) filters.

The FIR filters are implemented using equation

$$O(n) = \sum_{k=1}^{L} b(k)I(n-k) \quad (1)$$

Where $b(k)$ is the impulse response of the linear filter. The output of the filter, O(n), can be thought of as an estimate of the desired signal, $R(n)$. E(n),can be determined by simple subtraction of estimate and desired signal: $E(n) = R(n) - O(n)$.

The least mean square algorithm is used to error signal E(n) = $R(n) - O(n)$. Note that $O(n)$ is the output of the linear filter, $L(z)$. E(n) can be written as:

$$E(n) = R(n) - O(n) = R(n) - \sum_{k=1}^{L} b(k)I(n-k) \quad (2)$$

where L is the length of the FIR filter. In fact, it is the sum of $E(n)^2$ which is minimized, specifically:

$$\varepsilon = \sum_{n=1}^{N} E(n)^2 = \sum_{n=1}^{N}\left[R(n) - \sum_{k=1}^{L} b(k)I(n-k)\right]^2 \quad (3)$$

squaring the elements in the brackets, leads to a quadratic function of the FIR filter coefficients, b(k), in which two of the terms can be identified as the autocorrelation and cross correlation: ε=

$$\sum_{n=1}^{N}[R(n) - 2\sum_{k=1}^{L} b(k)r_{dx}(k)' + \sum_{k=1}\cdot\sum_{l=1}^{L}(b(k)b(l)r_{xx}(k-l) \quad (4)$$

where r_{dx} and r_{xx} are the autocorrelation and cross correlation. In order to Minimize the error function with respect to the FIR filter coefficients, we take derivatives with respect to $b(k)$ and set them to zero:

$\frac{\partial \varepsilon}{\partial b(k)} = 0$ which leads to

$$\sum_{k=1}^{L} b(k)r_{xx}(k-m) = r_{dx}(m) \quad \text{for } 1 \leq m \geq L \quad (5)$$

Equation (5) shows that the optimal filter can be derived knowing only the autocorrelation function of the input and the cross correlation function between the input and desired waveform.

Equation (5), represents a series of L equations that must be solved simultaneously to solve for the FIR coefficients. The matrix expression for these simultaneous equations is:

$$\begin{bmatrix} r_{xx}(0) & r_{xx}(1) & r_{xx}(L) \\ r_{xx}(1) & r_{xx}(0) & r_{xx}(L-1) \\ & . & \\ & . & \\ r_{xx}(L) & r_{xx}(L-1) & r_{xx}(0) \end{bmatrix} \begin{bmatrix} b(0) \\ b(1) \\ . \\ . \\ b(L) \end{bmatrix} = \begin{bmatrix} r_{dx}(0) \\ r_{dx}(1) \\ . \\ . \\ r_{dx}(L) \end{bmatrix} \quad (6)$$

Equation (6) is commonly known as the Wiener-Hopf equation and is a basic component of Wiener filter theory (Semmlow, 2004).

2.2Enveloped wavelet power spectrum:

In wavelet analysis, a variety of different probing functions may be used, but the family always consists of enlarged or compressed versions of the basic function, as well as translations. Mathematically, the wavelet transform of a finite energy signal x (t) with the analyzing wavelet ψ, leads to the definition of continuous wavelet transform as given in equation (7).

$$W(a, b) = \int_{-\infty}^{\infty} x(t)\frac{1}{\sqrt{|a|}}\psi*\left(\frac{t-b}{a}\right)dt \quad (7)$$

Where b (dilation parameter) acts to translate the function across x (t) and the variable a (scaling parameter) acts to vary the time scale of the wavelet function ψ . The $*$ indicates the operation of complex conjugate and the normalizing parameter $1/\sqrt{a}$ ensures that the energy is the same for all values of a.

The envelope detection or amplitude demodulation is the technique of extracting the modulating signal from an amplitude-modulated signal. The result is the time-history of the modulating signal. Envelope analysis is the FFT frequency spectrum of the modulating signal. The vibration signal of a faulty gear can be viewed as a carrier signal at a resonant frequency of the gear modulated by a decaying envelope. The goal of the enveloping approach is to replace the oscillation caused by each impact with a single pulse over the entire period of the impact. Laplace wavelet is a complex analytical and single sided damped exponential and is given in equation (8). The view of Laplace wavelet is shown in Figure 2

$$\psi(t) = A\, e^{-\left(\frac{\beta}{\sqrt{1-\beta^2}}+i\right)\omega_c t} \qquad t \geq 0$$

$$\psi(t) = 0 \qquad \text{t is otherwise} \qquad (8)$$

Where β is the damping factor that controls the decay rate of the exponential envelope in the time domain and hence regulates the resolution of the wavelet and it simultaneously corresponds to the frequency bandwidth of the wavelet in the frequency domain. The frequency ω_c determines the number of significant oscillations of the wavelet in the time domain and corresponds to wavelet center frequency in the frequency domain and A is an arbitrary scaling factor (Al-Raheem, 2007).

The optimal values of β and ω_c for given vibration signal can be found by adjusting the time-frequency resolution of the Laplace wavelet to the decay rate and the frequency of the impulses to be extracted. A high kurtosis values indicates high impulsive content of the signal with more sharpness in the signal intensity distribution

Let *x (n)* be a real discrete time random process, and WT_a its *N* point Laplace wavelet transform at scale a. The Laplace Wavelet Kurtosis (L*WK*) for *x(n)* is defined as the kurtosis of the magnitude of WT_a at each wavelet scale a as in the equation (9). (Al-Raheem, 2011)

$$LWK_{(a)} = \frac{\sum_{n=1}^{N} abs(WT_a{}^4(x(n), \psi_\beta, \omega_c))}{[\sum_{n=1}^{N} abs(WT_a{}^2(x(n), \psi_\beta, \omega_c))]^2} \qquad (9)$$

The Morlet wavelet is defined as given in equation (10) (Semmlow, 2004). The view of Morlet wavelet is shown in Figure 3

$$\psi(t) = e^{-t^2} \cos\left(\pi\sqrt{\frac{2}{\ln 2}}\ t\right) \qquad (10)$$

The wavelet transform (WT) of a finite energy signal x(t), with the mother wavelet ψ (t), is the inner product of x(t) with a scaled and conjugate wavelet ψ^* *a,b*. Since the analytical and complex wavelet is employed to calculate the wavelet transform, the result of the wavelet transform is also an analytical signal as shown in equation (11) and (12).

$$WT\{x(t), a, b\} = \langle x(t), \psi_{a,b}(t)\rangle = \frac{1}{\sqrt{a}} \int_{-\infty}^{\infty} x(t)\ \psi^*_{a,b}(t)dt \qquad (11)$$

$$= \mathrm{Re}\,[WT(a, b)] + i\mathrm{Im}\,[WT(a, b)] = A(a, b)\, e^{i\theta(a.b)} \qquad (12)$$

Where $\psi_{a,b}$ is a family of daughter wavelet, defined by the dilation parameter *a* and the translation parameter *b*, the factor $1/\sqrt{a}$ is used to ensure energy preservation. The time-varying function A(*a*, *b*) is the instantaneous envelope of the resulting wavelet transform (EWT) which extracts the slow time variation of the signal, and is given by equation (13)

$$A(a,b) = EWT(a,b) = \sqrt{\{\mathrm{Re}[WT(a,b)]\}^2 + \{\mathrm{Im}[WT(a,b)]\}^2} \qquad (13)$$

For each wavelet, the inner product results in a series of coefficients which indicate how close the signal is to that particular wavelet. To extract the frequency content of the enveloped correlation coefficients, the wavelet-scale power spectrum (SWPS) (energy/unit scale) is given by equation (14)

$$SWPS\ (a, \omega) = \int_{-\infty}^{\infty} |SEWT(a,\omega)|^2 d\omega \qquad (14)$$

Where SEWT (a, ω) is the Fourier transform of EWT (a,b).The total energy of the signal x (t) is given in equation

$$TWPS = \int |x(t)|^2 dt = \frac{1}{2\pi} \int_{-\infty}^{\infty} SWPS(a,\omega)da \qquad (15)$$

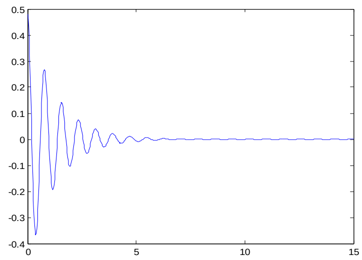

(a)

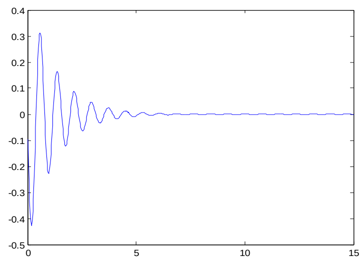

(b)

Figure 2. Laplace wavelet (a) Real part of Laplace wavelet (b) Imaginary part of Laplace wavelet

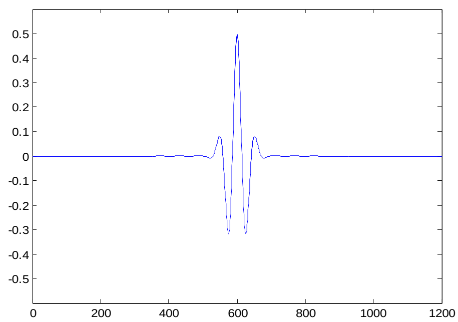

Figure 3. Morlet wavelet

III Experimental setups and procedure:

Experimental setup1:The fault simulator 1is depicted in Figure 4. The experimental setup consists of single stage gear box, motor, loading system, coupling and bearings. One gear was connected to 0.5 HP, 2900 RPM electric motor through coupling and the other gear was connected to a loading system. The gear and pinion has 46 and 23 teeth respectively. The shafts of 25mm diameter connect gears with motor and loading system. The shafts are supported at its ends through bearings. The vibration data is collected from the drive end bearing of gear box using the accelerometer (model 621B40, IMI sensors, sensitivity is 1.02 $mV/m/s^2$ and frequency range up to 18 kHz) with a NI Data Acquisition Device (NI-DAQ-National Instruments-NI SCXI-1000 chassis through SCXI-1530-channel 0, SCXI-1530-channel 1 and SCXI-1530-channel 2).The view of healthy gears is shown in Figure 5. The collected Vibration data are exported as data file to MATLAB software package for further processing.

Figure 4. Fault Simulator set up 1

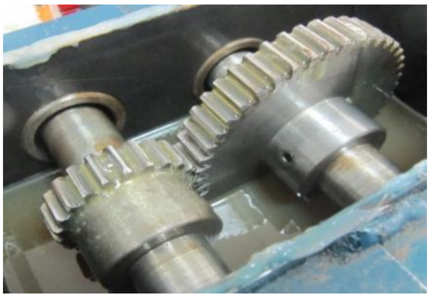

Figure 5. View of healthy gears

In the experimental investigation, the vibration signal was collected from a healthy gear at shaft speed of 2850 RPM under constant load condition. The Gear mesh frequency (GMF) is calculated to be 23*2850/60 =1092.5Hz. Further faults are induced in three different stages as shown in Table 1 and the corresponding vibration readings were taken. The views of faulty gear are shown in Figure 6. The sampling frequency of 16,000 Hz was used to collect the data for 2.4 seconds. The data was collected from the setup after reaching the required speed.

Stage	Condition of the gear	Fault description
Stage 0	Healthy gear	Without any induced fault
Stage 1	Faulty gear	A crack of 3mm is induced at the root of the tooth
Stage 2	Faulty gear	Tooth was partially broken
Stage 3	Faulty gear	Tooth was completely removed

Table 1: Stages of induced fault for Fault Simulator set up 1.

(a)

(b)

(c)

Figure 6.Gears with induced fault in 3 stages. (a) Stage 1. (b) Stage 2.(c) Stage 3.

Experimental setup2:

The fault simulator 2 is depicted in Figure 7. The experimental setup consists of variable speed motor, single stage gear box, couplings, belt & pulleys, loading system, and bearings. The electric motor of capacity 0.5 HP and variable speed maximum up to 10,000RPM is connected to one gear of the gear box through coupling and belt & pulleys system and the other gear is connected to a loading system. The gear and pinion has 30 and 20 teeth respectively. The steel shafts of 5/8” diameter connect gears with motor and loading system. The shafts are supported through bearings. The vibration data is collected from the drive end bearing of gear box using the accelerometer with a NI Data Acquisition Device. The views of healthy and faulty gears are shown in Figure 8. The collected Vibration data are exported as data file to MATLAB software package for further processing.

In the experimental investigation, the vibration signal was collected from a healthy gear at shaft speed of 900RPM under constant load condition. The Gear mesh frequency (GMF) is calculated to be 20*900/60 =300Hz. Further faults were induced in two different stages as shown in Table 2 and the corresponding vibration readings were taken. The sampling frequency of 16,000

Hz was used to collect the data for 2 seconds. The data was collected from the setup after reaching the required speed.

Figure7. Fault Simulator set up 1.

(a)

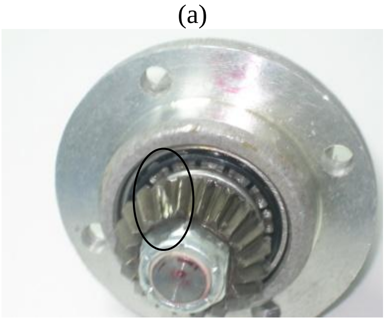

(b)

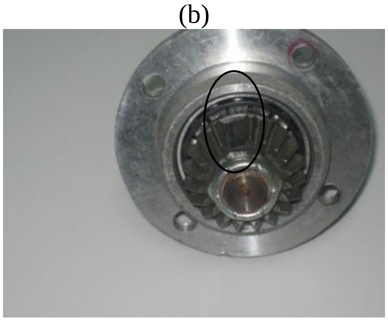

(c)

Figure 8. Gears with induced fault in 2 stages. (a) Stage 0. (b) Stage 1.(c) Stage 2.

Stage	Condition of the gear	Fault description
Stage 0	Healthy gear	Without any induced fault
Stage 1	Faulty gear	The chipped tooth
Stage 2	Faulty gear	Tooth was completely removed

Table 2. Stages of induced fault for Fault Simulator set up 2

IV Implementing of wavelet power spectrum

To visualize the performance of the proposed approach, this section presents several application examples for the detection of localized gear fault. It is well known that the most important components in gear vibration spectra are the tooth meshing frequency and its harmonics, together with sidebands due to modulation phenomena. The increment in the number and amplitude of sidebands indicate a fault condition. The methodology of implementing envelope power spectrum is shown in Figure 9. A typical time domain signal obtained from the experimental setup with gear fault, using accelerometer is given in Figure 10.This is further processed using various signal processing techniques like wavelet enveloped power spectrum based on Morlet wavelet and Laplace wavelet. Wiener filter technique was used to enhance the signal components before it is processed using enveloped power spectrum. The GMF and its side bands are represented in various power spectrums with indication of data cursor value.The rotational frequency of pinion, gear, GMF and side bands of GMF are depicted in Table 3 for both the experimental setups.

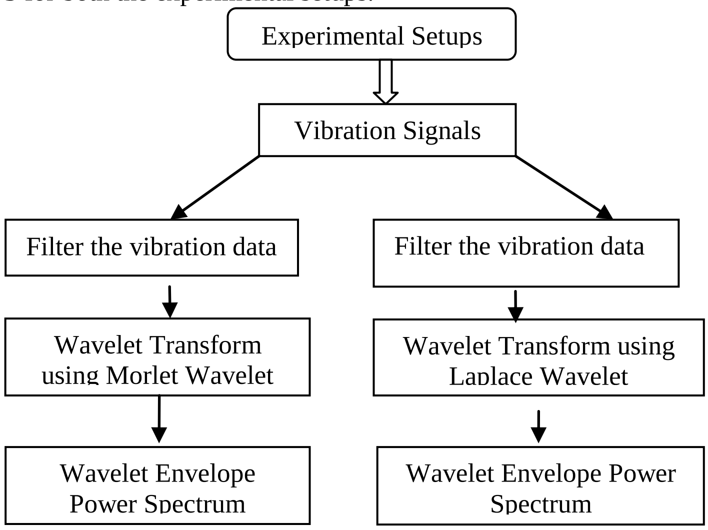

Figure 9. Methodology of implementing envelope power spectrum

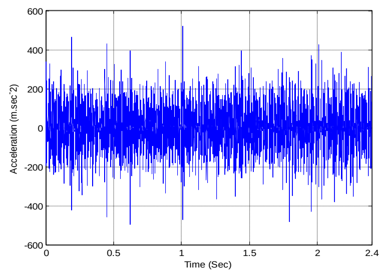

Figure 10.Time domain signal of gear with fault

Description	Experimental set up 1(Frequency)	Experimental set up 2(Frequency)
Pinion rotational frequency	48	15
Gear rotational frequency	24	10
GMF	1093	300
Sideband frequency at GMF	1045	285
Side band frequency at GMF	1140	290

Table 3. Frequency of rotation

4.1 Laplace wavelet enveloped Power Spectrum for experimental set up 1

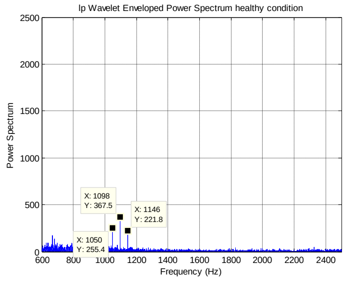

(a)

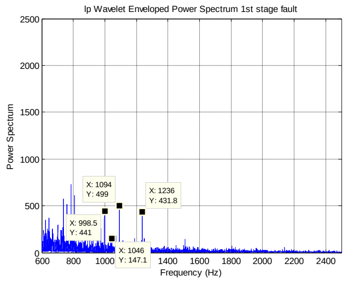

(b)

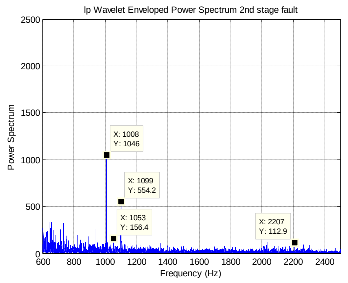

(c)

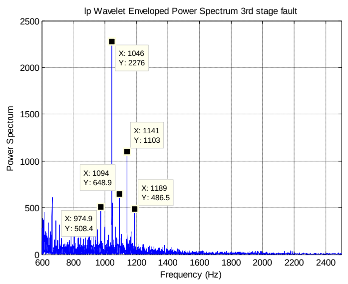

(d)

Figure 11.*Laplace wavelet enveloped* Power Spectrums for *experimental set up 1*. (a) Without any defect. (b) 1st stage of defect. (c) 2nd stage of defect (d) 3rd stage of defect

Laplace wavelet enveloped power spectrums are developed using the data from the experimental set up1 for the healthy and faulty gear in three different stages of fault are shown in Figure 11(a) to 11(d) respectively. As seen in spectrums, vibration amplitude at GMF is increasing in line with the severity of fault from 367.5 to 648 mm/s^2 with dominant sidebands, indicating severity of fault. Side band level remains low as seen in Figure 11(a), for a gear box in good condition. Laplace wavelet based enveloped power spectrums analysis is powerful in isolating peaks at sidebands of GMF, which can provide more precise information about defect condition.

4.2 Laplace wavelet enveloped Power Spectrum for experimental set up 2

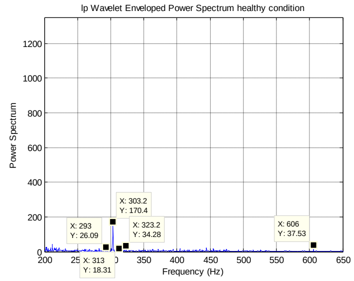

(a)

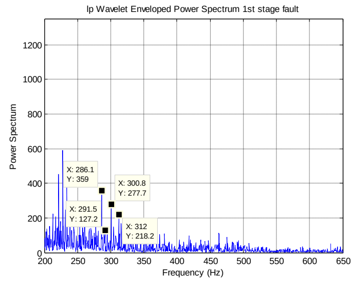

(b)

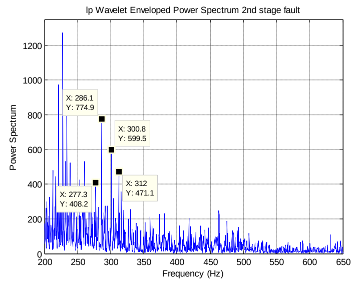

(c)

Figure 12.*Laplace wavelet enveloped* Power Spectrums for *experimental set up 1*. (a) Without any defect. (b) 1st stage of defect. (c) 2nd stage of defect

Figure 12 (a) to 12(d) depicts the Laplace wavelet enveloped power spectrums of the experimental set up2 data for the healthy gear and for faulty gear in two different stages of fault. As seen in Laplace wavelet based enveloped power spectrums, vibration amplitude at GMF is increasing in line with the severity of fault from 170 to 599 mm/s^2 with dominant sidebands. Side bands in the spectrum indicate the severity of the fault. For a gear box in good condition, side band level remains low as seen in Figure 12(a). The side bands rising with the severity of the fault is shown in the spectrums.

4.3Morlet wavelet enveloped Power Spectrum for experimental set up 1

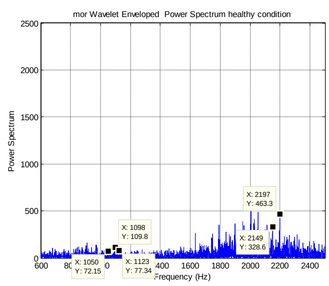

(a)

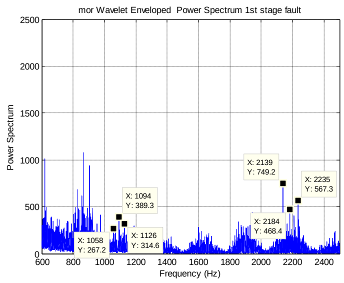

(b)

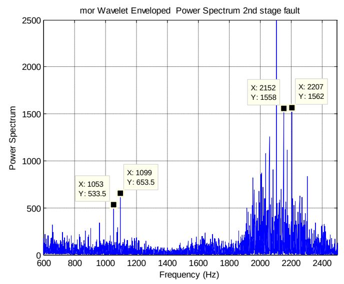

(c)

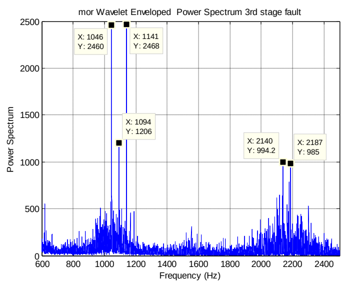

(d)

Figure 13.*Morlet wavelet enveloped* Power Spectrums for *experimental set up 1*. (a) Without any defect. (b) 1st stage of defect. (c) 2nd stage of defect (d) 3rd stage defect

Morlet wavelet enveloped power spectrums for the experimental set up1data are shown for the healthy gear in Figure 13(a) and for 3 induced stages of faults in Figure 13(b) – 13(d). Amplitude of GMF is increasing from 109 to 1206 mm/s^2 for healthy gear and faulty gear in 3 different stages. Vibration amplitude of side bands is significant. Changes in the number and strength of the side bands indicate severity of fault.

4.4 Morlet wavelet enveloped Power Spectrum for experimental set up 2:

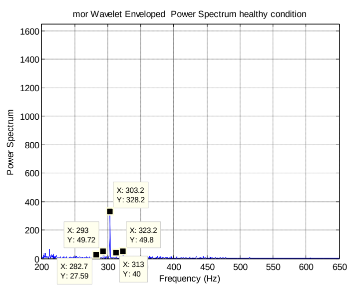

(a)

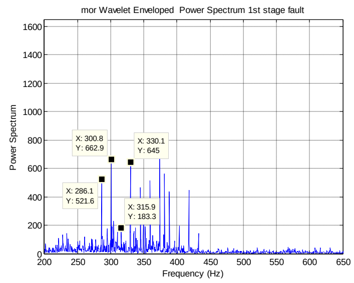

(b)

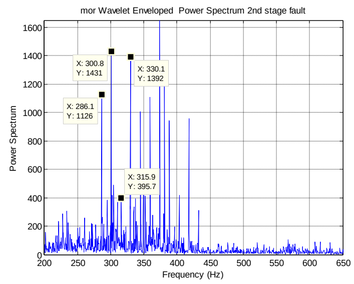

(c)

Figure 14.*Morlet wavelet enveloped* Power Spectrums for *experimental set up 2*. (a) Without any defect. (b) 1st stage of defect. (c) 2nd stage of defect

The vibration data from the experimental set up 2 are used to develop the Morlet wavelet enveloped power spectrums and the corresponding spectrums are shown for the healthy gear in Figure 14(a) and for 3 induced stages of faults in Figure 14(b) – 14(d). Amplitude of GMF is increasing from 328to 1431 mm/s^2 for healthy gear and faulty gear in 2 different stages. The significant increase in amplitude of side bands above the GMF amplitude indicates the severity of fault.

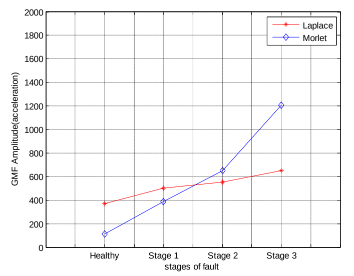

(a)

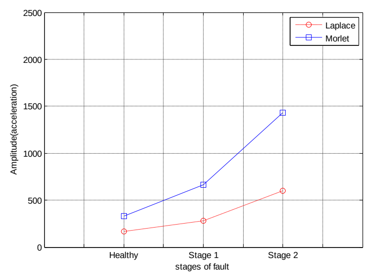

(b)

Figure15. Vibration amplitude at GMF (a) Experimental set up 1 (b) Experimental set up 2

Figure 15 shows the variation in vibration amplitude at GMF for the experimental setups. The increase in amplitude is depicted with the corresponding increase in severity of fault. Morlet enveloped power spectrum shows considerable increase in amplitude.

V Conclusions

Different types of signal processing methods adopted using wavelet transform for the gear fault diagnosis is presented in this paper. Gear fault diagnosis using Laplace wavelet and Morlet wavelet enveloped power spectrum is implemented and the results are studied for the various stages of induced fault conditions in the experimental setups. Wiener filter is used to enhance the fault signal components, which support for the early detection of the fault.

From the studies conducted both Morlet and Laplace wavelet based enveloped power spectrum depicts significant increase in magnitude of vibration amplitude at GMF along with increase in the size of fault. Further, the study shows significant change of trend in vibration amplitude at GMF and X × RPM sideband of GMF along with increase in the size of fault and hence shows prominence as a useful tool to show the correlation between healthy and faulty gears. It was also observed that change of trend in vibration amplitude at GMF and 1× RPM sideband of GMF from the Morlet wavelet analysis compared to the Laplace wavelet. However, Laplace wavelet analysis is more powerful in isolating peaks at multiple RPM sidebands of GMF which can provide more precise information about defect condition. All these factors enhance the use of this proposed method for gear fault diagnosis

Reference:

[i] Wandel J.. 2006. Multistage gearboxes: Vibration based quality control, KTH Engineering Sciences, Stockholm, Licentiate Thesis,TRITA-AVE 2006:27 ISSN 1651-7660.

[ii] Abu-Mahfouz I.A., 2007. Gearbox health monitoring experiment using vibration signals. Journal of Engineering Technology, Vol.24, No. 1, pp. 26-31.

[iii] Omar F.K. and Gaouda A.M.,2009. Gearbox diagnostics using wavelet based windowing technique. Journal of Physics:Conference Series, Vol. 181, No. No. 1, Conf. Ser. 181 012089

[iv] K.P.Ramachandran, Khalid Fathi & B.K.N. Rao(2010), Recent trends in systems performance monitoring & failure diagnosis. The IEEE International conference on industrial engineering & engineering management, 7-

[v] Lin J, Zuo M.J., 2003. Gear box fault diagnosis using adaptive wavelet filter, Mechanical Systems And Signal Processing, Vol. 17,No. 6, pp. 1259-1269.

[vi] Saravanan N. Ramachandran K.I.,.2010. Incipient gear box fault diagnosis using discrete wavelet transform for feature extraction and classification using artificial neural network. An international journal of Expert Systems with Applications, Vol. 37, pp.4168-4181.

[vii]Choy F.K., Huang, J.J., Zakrajsek R.F, Handschuh T.P, Townsend.1994. Vibration signature of a faulted gear transmission system.NASA, Technical Memorandum 106623, Technical Report ARL-TR-475 AIAA-94-2937.

[vii] Dalpiaz G., Rivola A. And Rubini R.,1998. Gear fault monitoring: comparison of vibration analysis techniques. Proceedings of the 3rd International Conference on Acoustical and Vibratory Surveillance Methods and Diagnostic Techniques, Vol. 13, pp, 623-637.

[ix] Randall R.B. 1982. A new method of modeling gear faults. Journal of Mechanical Design, Vol. 104, pp. 259-267.

[x] Pan M.C., Sas P., 1996. Tansient analysis on machinery condition monitoring. International Conference on Signal Processing,Proceedings, ICSP 2, pp. 1723-1726.

[xi] Peng Z.K., Chu F.L., 2004. Application of the wavelet transform in machine condition monitoring and fault diagnostics: a review with bibliography. Mechanical Systems and Signal Processing, Vol. 18, No. 2, pp. 199–221.

[xii] Purushotham V., Narayanan S, and Suryanarayana, Prasad A.N., 2005 Multi-fault diagnosis of rolling bearing elements using wavelet analysis and hidden Markov model based fault recognition. NDT & E International Vol. 38, No. 8, pp. 654-664.

[xiii] Shi D.F., Wang W.J. and Qu L.S., 2004. Defect detection for bearing using envelope spectra of wavelet transform. ASME J of Vibration and Acoustics, Vol. 120, pp. 567-574.

[xiv] Nikolaou N.G and Antoniadis I.A., 2002. Demodulation of vibration signals generated by defects in rolling element bearings using complex shifted Morlet wavelets. Mechanical Systems and Signal Processing, Vol. 16, No. 4, pp. 677-694.

[xv]Junsheng C., Dejie Y., Yu Y., 2005. Application of an impulse response wavelet to fault diagnosis of rolling bearings, Mechanical Systems and Signal Processing, Vol. 21, No. 2, pp. 920–929.

[xvi]Al-Raheem K.F, Roy. A, Ramachandran.K.P. 2006. Detection of rolling element bearing faults using optimized –wavelet denoising technique. International Conference on Signal Processing, Beijing, China.

[xvii]Al-Raheem K.F., Roy A., Ramachandran K.P, Harrison D.K., Grainger S., 2009, International Journal of Advanced Manufacturing Technology, Vol. 40, pp. 393-402.

[xviii] Al-Raheem K.F., Roy A., Ramachandran K.P, Harrison D.H., Grainger, S. 2007. Rolling element gearing fault diagnosis using Laplace-wavelet envelop power spectrum. EURASIP Journal on Advances in Signal Processing, Vol. 2007, article id 73629, 14pages

[xix] Yanyang Z., Xuefeng C. Zhengila H. And Peng C., 2005. Vibration based modal parameters identification and wear fault diagnostics using Laplace wavelet. Key Engineering Materials, Vol. 293-294, pp. 183-190.

[20] Freudinger L.C., Lind R., and Brenner M.J., 1998. Correlation filtering of modal dynamics using the Laplace wavelet. Proceeding of the 16th International Modal Analysis Conferences, Vol. 2, pp. 868-877.

[xx] J. Lin, L. Qu, Feature extraction based on Morlet wavelet and its application in mechanical fault diagnosis, Journal of Sound and Vibration 234 (2000) 135–148.

[xxi] J. Lin, M.J. Zuo, K.R. Fyfe, Mechanical fault detection based on the wavelet de-noising technique, Journal of Vibration and Acoustics 126 (2004) 9–16.

[xxii] H. Qiu, J. Lee, J. Lin, G. Yu, Wavelet filter-based weak signature detection method and its application on rolling element bearing prognosis, Journal of Sound and Vibration 289 (2006) 1066–1090.

[xxiii] H. Qiu J. Lee, J. Lin, G. Yu, Robust performance degradation assessment methods for enhanced rolling element bearing prognostics, Advanced Engineering Informatics 17 (2003) 127–140.

[xxiv] J. Lin, M.J. Zuo, Gearbox fault diagnosis using adaptive wavelet filter, Mechanical Systems and Signal Processing 17 (2003)1259–1269.

[xxv] N.G. Nikolaou, I.A. Antoniadis, Demodulation of vibration signals generated by defects in rolling element bearings using complex shifted Morlet wavelets, Mechanical Systems and Signal Processing 16 (2002) 677–694.

[xxvi] D.L. Donoho, De-noising by Soft-Thresholding, IEEE Transactions on Information Theory 41 (1995) 613–627.

[xxviii] D.L. Donoho, I.M. Johnstone, Ideal spatial adaptation via wavelet shrinkage, Biometrika 81 (1994) 425–455.

[xxix] S. Mallat, A Wavelet Tour of Signal Processing, Academic Press, San Diego, 1998.

[xxx] R.M. Rao, A.S. Bopardikar, Wavelet Transforms: Introduction to Theory and Application, Addison Wesley, Reading, MA, 1998.

[xxxi] Al-Raheem K.F., Kareem W.A., 2011..Rolling element bearing fault diagnostics using Laplace wavelet kurtosis, IJMSE, World Academic Publishing, Vol.1 No.1, pp. 17-25.

[xxxii] I Soltani Bozchalooi, Ming Liang.,2007..A joint resonance frequency estimation and in-band noise reduction method for enhancing the detectability of bearing fault signals

[xxxiii] Khalid Al.Raheem, Ashok roy, K.P.Ramachandran," performance evaluation of adaptive noise canceller and adaptive line enhancer for the application of rolling element bearing fault detection" 19th International congress, COMADEM 2006, kumar, pratibha and Rao (Eds), lulea, Sweden, ISBN: 978-91-631-8806-0.

[xxxiv] F.Combet, L.Gelman.,2009..Optimal filtering of gear signals for early damage detection based on the spectral kurtosis.
[xxxv] Semmlow J.L. 2004. Bio signal and biomedical image processing, Marcel Dekker, Inc. New York, USA, ISBN0-8247-4803-4.

Authors profile:

Mr.M.Lokesha received his B.E. degree in Mechanical Engineering from Mysore University, Mysore, India in 1989 and M.TECH. Degree in Maintenance engineering from Mysore University, Mysore, India in 1994. Presently, he is working as a Senior Lecturer in the Department of Mechanical and Industrial Engineering at Caledonian College of Engineering, Muscat. He has been working for 22 years in engineering institutions His research focuses on vibration instrumentation & measurement, condition monitoring of rotating machinery. He is currently PhD research student at National Institute of Technology, Durgapur, India.

Dr. Manik Chandra Majumdar is a Professor in the Department of Mechanical Engineering and Member, Board of Governors of NIT Durgapur India. He has a PhD from the Indian Institute of Technology, Kharagpur, India. He has guided many Ph.D. scholars. His prime area of research is Tribology /Design & Production

Dr. K. P. Ramachandran B.E, M.Tech, PhD is currently working as Associate Dean (Post Graduate Studies & Research), Caledonian College of Engineering,Muscat, Sultanate of Oman. He has been working for more than 25 years in engineering institutions and as a consultant for many industries. He has research interest in the vibration instrumentation & measurement, analysis and control, condition monitoring of rotating machinery. He has many publications to his credit and has been conferred Sir C.V. Raman award for the best technical paper published in the Journal of Vibration & Acoustics (1997). He is on the editorial board and technical reviewer for many international journals and conferences. He has guided many PhD students in the area of condition monitoring and maintenance management.

Dr.Khalid Fatihi Abdul-Raheem, B.E., M.Tech from University of Technology, Iraq and PhD from Glasgow Caledonian University, UK. Presently he is working as a Associate professor in the Department of Mechanical Engineering at Sohar University, Sohar,Oman. He has been working for more than 22 years in engineering institutions and many industries. He has many publications to his credit. He has research interest in condition monitoring and signal analysis, artificial intelligence, automatic control system, mechanical vibration analysis and control.